Periodica Polytechnica
Civil Engineering

60(3), pp. 427–436, 2016
DOI: 10.3311/PPci.7933

RESEARCH ARTICLE

Some Aspects of Support Stiffness Effects on Dynamic Ballasted Railway Tracks

Seyed-Ali Mosayebi, *Jabbar-Ali* Zakeri, *Morteza* Esmaeili

Received 26-01-2015, revised 23-08-2015, accepted 13-01-2016

Abstract

The railway track technical literature lacks proper reports on the key effects of the support stiffness on the track behavior with various sleeper geometries. Hence, it is the aim of this research to report on the assessment of the track foundation stiffness. The pyramid model equations are developed for three different stress conditions including WOA model for the cases without stress overlap area in the adjacent sleepers, OAP for considering the stress overlap area between adjacent sleepers with pyramid distribution and OAC for the cases of stress overlap area between adjacent sleepers with cubical stress distribution. A vehicle/track interaction problem studied using the finite element method. The vehicle is considered as a series of moving masses with three degrees of freedom corresponding to the carbody, the bogie and the wheelset masses. The track is considered as beam elements resting on the viscoelastic foundation. The results of the numerical analyses of the vehicle/track system are presented as ratios of the railway track vertical displacement to the vehicle axle load for various foundation stiffness. Many correlation equations are suggested that interconnect the track stiffness with variables such as the ballast depth, the sleeper width, and the sleeper distance.

Keywords

Ballasted Railway Track · Support Stiffness · Pyramid model · Sleeper Geometries

Seyed-Ali Mosayebi
School of Railway Engineering, Iran University of Science and Technology, Tehran, Iran
e-mail: mosayebi@iust.ac.ir

Jabbar-Ali Zakeri
The Center of Excellence in Railway Transportation, School of Railway Engineering, Iran University of Science and Technology, Tehran, Iran
e-mail: zakeri@iust.ac.ir

Morteza Esmaeili
The Center of Excellence in Railway Transportation, School of Railway Engineering, Iran University of Science and Technology, Tehran, Iran
e-mail: m_esmaeili@iust.ac.ir

1 Introduction

The worldwide rising demand for the passenger and the cargo transportation has captured the attention of railway operators and triggered the need for further development within the industry. Railway transportation is safer, more cost effective and environmentally consistent compared with the other modes of transport. The railway track analysis is the field of interest to many researchers. As some examples, Szépe [1] studied the railway superstructure as a beam on the elastic foundation. Zakeri and Xia [2] investigated the railway parameters due to the moving train loads. Zoller and Zobory [3] investigated the track model for metro due to the moving load. Amongst the most important issues in this mode of transportation is its safety that is considerably under the influence of the track quality. Generally speaking, the railway track quality depends on the track stiffness. In the case of the ballasted track, the track stiffness remarkably relates to various parameters such as the ballast depth, the sleeper width and the distance of the sleepers. This factor has been investigated by various researchers through analytical and experimental approaches. Kerr [4, 5] investigated the measuring methods of railway track stiffness. One of the methods for calculating the support stiffness in the railway tracks is the pyramid model developed by Zhai et al. [6]. Puzavac et al. [7] studied the effect of track stiffness due to moving load. Breul and Saussine [8] studied the mechanical specifications of the railway ballast in situ. Moreover, Zakeri and Abbasi [9] and Zakeri et al. [10] investigated the support modulus of railway track in field tests. In another study, Esmaeili et al. [11] investigated the support stiffness on train induced vibrations in desert land. Reviewing the existing literature indicates that the less researches have been done on the effects of the support stiffness on the vehicle/track interaction specifically by considering the important parameters such as the ballast depth, sleeper width and the distance of sleepers. In the present study, at the first stage, the existing pyramid model that was developed by Zhai et al. [6] is extended to three different stress conditions including WOA for the cases without stress overlap area in adjacent sleepers, OAP for considering the stress overlap area between adjacent sleepers with pyramid stress distribution and OAC for the cases of stress overlap area between adjacent sleepers with cubical stress distribution. In the next stage, a vehicle/track problem is simulated using finite element method. In this regard, the results of the developed computer code are verified by comparing with numerical results of Lei and Zhang [12] and Koh et al. [13]. Finally, comprehensive sensitivity analyses are performed on the effectiveness of the various parameters on the track stiffness. Consequently, many correlation equations are proposed for the ballast depth, sleeper widths, sleeper distances and the ratio of the railway track vertical displacement to the vehicle axle load.

2 Derivation of the individual support stiffness in railway track

The transfer of the train load from a sleeper to the ballast layer is based on the assumption of pyramid distribution [6, 14]. Therefore, the vibrating section of the ballast under each sleeper is as a pyramid shape. In a pyramid model, parameters such as the ballast density ρ_b, ballast depth h_b, support length of half sleeper L_e, width of sleeper L_b, distance between sleepers L_s, elasticity modulus of ballast E_b and stress distribution angle of the ballast α are effective. In this model, the ballast stresses are distributed throughout the pyramid shape [6]. Fig. 1 presents schematic of the ballasted track without stress overlap area with adjacent ballast layers.

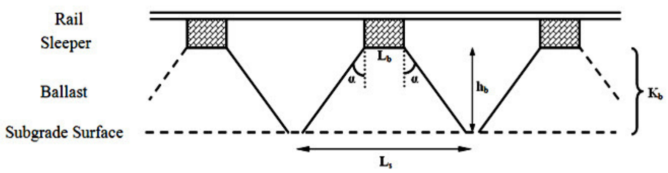

Fig. 1. The ballasted track without stress overlap area

In this figure, h_b is the total depth of the ballast layer. The transmitted force from a sleeper to the ballast layer is estimated as follows:

$$Q = qL_bL_e \tag{1}$$

In this equation, Q and q are the force and the stress under sleeper, respectively. Therefore, the force and the strain in the depth of z in the ballast layer are calculated as follows:

$$Q = q_z\,(L_b + 2z\tan\alpha)\,(L_e + 2z\tan\alpha) \tag{2}$$

$$\varepsilon_z = \frac{q_z}{E_b} \tag{3}$$

In this equation, q_z and ε_z are the stress and the strain in the depth of z in the ballast layer, respectively. Consequently, the settlement (S) and the individual support stiffness (K_b) in the ballasted railway track without stress overlap area are calculated as follows:

$$S = \int_0^{h_b} \varepsilon_z dz = \int_0^{h_b} \frac{q_z}{E_b} dz \tag{4}$$

$$\begin{aligned} K_b &= \frac{Q}{S} = \\ &= \frac{2\,(L_e - L_b)\tan\alpha}{\ln\left[(L_e/L_b)\,.\,(L_b + 2h_b\tan\alpha)\,/\,(L_e + 2h_b\tan\alpha)\right]} E_b \end{aligned} \tag{5}$$

If the distance between the sleepers is small or the depth of the ballast layer is high, the overlap in the stress distribution area takes place. Fig. 2 shows a ballasted track with stress overlap area [6].

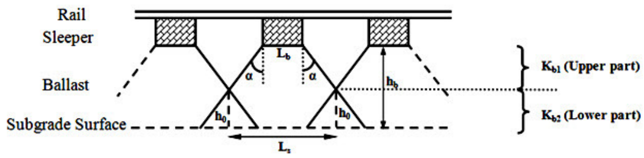

Fig. 2. The ballasted track with stress overlap area

In this figure, h_b and h_0 are the depth of the ballast and the overlap area with adjacent ballast layer, respectively [6]. The depth of the stress overlap area is determined as follows:

$$h_0 = h_b - \frac{L_s - L_b}{2\tan\alpha} \tag{6}$$

Consequently, the individual support stiffness in the ballasted track is calculated by the series combination of the upper and the lower parts stiffness as follows:

$$K_b = \frac{K_{b1}K_{b2}}{K_{b1} + K_{b2}} \tag{7}$$

In this equation, K_{b1} and K_{b2} are the stiffness of the upper and the lower parts of the ballast layer, respectively. The stiffness of the upper ballast layer, K_{b1}, is calculated based on Eq. (8).

$$K_{b1} = \frac{2\,(L_e - L_b)\tan\alpha}{\ln\left[(L_eL_s)\,/\,(L_b\,(L_e + L_s - L_b))\right]} E_b \tag{8}$$

For calculating the support stiffness in the lower part of the ballast layer, K_{b2}, two cases may be considered. These cases are: a) The support stiffness in the stress overlap area with the pyramid distribution b) The support stiffness in the stress overlap area with the cubical distribution. In what follows, both cases are investigated and their support stiffness is derived.

2.1 Stress distribution in stress overlap area with Pyramid distribution ($\beta \neq 0$)

Generally, distribution of the stress in the overlap area of the adjacent sleepers is as a pyramid shape. Fig. 3 presents a pyramid stress distribution in the overlap area.

In this case, the settlement of the ballasted track in the stress overlap area (S_{b2}) is calculated as follows:

$$S_{b2} = \frac{q\,L_s\,(L_e + L_s - L_b)}{E_b}\frac{1}{L_s}\frac{1}{2\tan\beta}\ln\left(1 + \frac{2h_0\tan\beta}{L_e + L_s - L_b}\right) \tag{9}$$

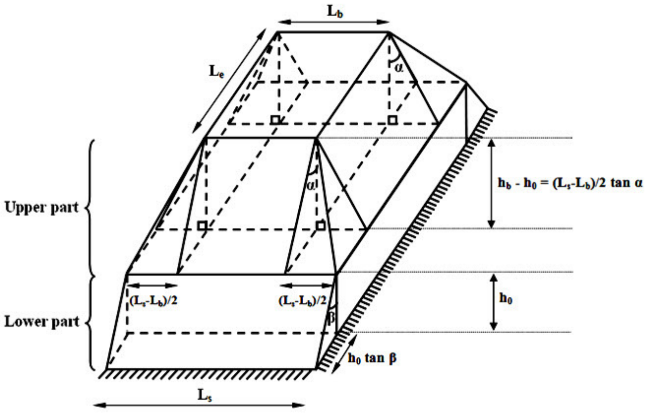

Fig. 3. A pyramid stress distribution pattern in the overlap area

Consequently, the stiffness of K_{b2} in the stress overlap area is derived as follows:

$$K_{b2} = \frac{2E_b L_s \tan\beta}{\ln\left(1 + \frac{2h_0 \tan\beta}{L_e + L_s - L_b}\right)} \tag{10}$$

By using the Eq. (6) and assuming $\alpha = \beta$, Eq. (10) can be presented as follows:

$$K_{b2} = \frac{2E_b L_s \tan\alpha}{\ln\left(\frac{L_e + 2h_b \tan\alpha}{L_e + L_s - L_b}\right)} \tag{11}$$

2.2 Stress distribution for the special case with Cubical distribution ($\beta = 0$)

The derived Eqs. (10) and (11) are in general forms and are suitable for the calculation of the ballasted track stiffness. When the distribution angle β tends to zero, Eq. (10) gives an ambiguous value for the track stiffness. As shown in Fig. 4, for $\beta = 0$, a cubical stress distribution pattern occurs in the overlap area. Such a condition usually happens in the ballast mixed with clay particles and signifies the punching shear failure of foundation [15]. In this special case, the stiffness that is given in Eq. (10) is modified as follows:

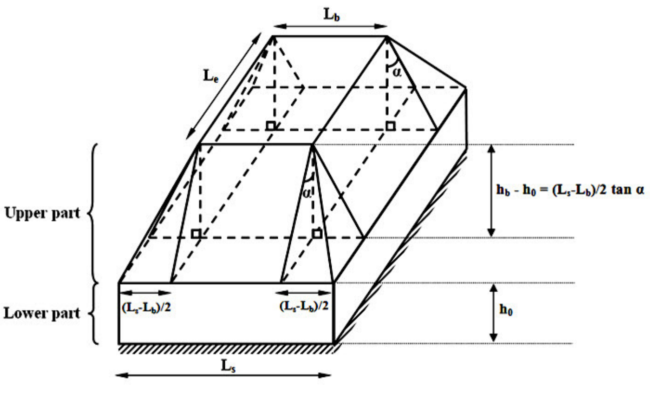

Fig. 4. A cubical stress distribution pattern in the overlap area

$$S_{b2} = \int_0^{h_0} \frac{q_z}{E_b} dz = \\ = \left(\frac{Q}{E_b L_s (L_e + L_s - L_b)}\right)\left(\frac{2h_b \tan\alpha - L_s + L_b}{2\tan\alpha}\right) \tag{12}$$

$$K_{b2} = \frac{Q}{S_{b2}} = \frac{E_b L_s \tan\alpha (2L_e + 2L_s - 2L_b)}{L_b - L_s + 2h_b \tan\alpha} \tag{13}$$

Therefore, for calculating the support stiffness, there are generally two equations for calculating K_{b2} in the stress overlap area. Table 1 shows all derived equations for calculating the individual support stiffness in railway track.

3 Comparison of the derived support stiffness for various conditions

In this section, the values of the support stiffness for various conditions are calculated and compared. In this regard, these equations are estimated for different ballast depths and various sleeper distances. The assumptions are: $\rho_b = 1800\,\mathrm{kg/m^3}$, $L_e = 0.95\,\mathrm{m}$, $L_b = 0.273\,\mathrm{m}$, $L_s = 0.6\,\mathrm{m}$, $\alpha = 35^o$, and $E_b = 100\,\mathrm{MPa}$. Fig. 5 illustrates the estimated support stiffness for the different depths of the ballast layers.

From Fig. 5 it can be observed that the individual support stiffness in the ballasted track reduces by increasing the ballast depths. Also, by decreasing the ballast depths, the results converge to a uniform value. The regression equations of the support stiffness with the ballast depths are presented in Table 2.

Fig. 6 depicts the calculated support stiffness for various distances of sleepers based on the developed models. In this regard, the adopted values for input parameters are as $\rho_b = 1800\,\mathrm{kg/m^3}$, $L_e = 0.95\,\mathrm{m}$, $L_b = 0.273\,\mathrm{m}$, $h_b = 0.45\,\mathrm{m}$, $\alpha = 35^o$, and $E_b = 100\,\mathrm{MPa}$.

From Fig. 6, it is suggested that the individual support stiffness in the railway track for the cases without stress overlap areas (WOA) remains constant while it increases by increasing the distance of sleepers in other cases. Also, with increasing the distance of sleepers, the results converge to a uniform value. The regression equations of the estimated support stiffness according to the distance of the sleepers are presented in Table 3.

In the next section, the individual support stiffness in the railway track for various sleeper geometries is calculated.

4 Calculation of the individual railway support stiffness for various sleeper geometries

The results in the previous section of this article prove significant variations of the individual railway support stiffness by changing the ballast depth and the distance of the sleepers. It can then be a valuable exercise to check on such variations based on the various sleeper geometries. Based on the leaflet No. 301 of Iran railway trasportation regulations, the width of the sleepers varies between 220 to 300 mm and the distance of the sleepers

Tab. 1. The derived individual support stiffness in the railway track for different conditions

Conditions	Symbols	Derived Stiffness	
Without stress overlap area	WOA	$K_b = \frac{2(L_e - L_b)\tan\alpha}{\ln[(L_e / L_b).(L_b + 2h_b \tan\alpha) / (L_e + 2h_b \tan\alpha)]} E_b$	
With stress overlap area $\beta \neq 0$	OAP	Stiffness of the upper part in the pyramid	$K_{b1} = \frac{2(L_e - L_b)\tan\alpha}{\ln[(L_e L_s) / (L_b(L_e + L_s - L_b))]} E_b$
(Pyramid stress distribution)		Stiffness of the lower part in the pyramid	$K_{b2} = \frac{2L_s \tan\alpha}{\ln\left(\frac{L_e + 2h_b \tan\alpha}{L_e + L_s - L_b}\right)} E_b$
With stress overlap area $\beta = 0$	OAC	Stiffness of the upper part in the pyramid	$K_{b1} = \frac{2(L_e - L_b)\tan\alpha}{\ln[(L_e L_s)/(L_b(L_e + L_s - L_b))]} E_b$
(Cubical stress distribution)		Stiffness of the lower part in the pyramid	$K_{b2} = \frac{L_s(2L_e + 2L_s - 2L_b)\tan\alpha}{L_b - L_s + 2h_b \tan\alpha} E_b$

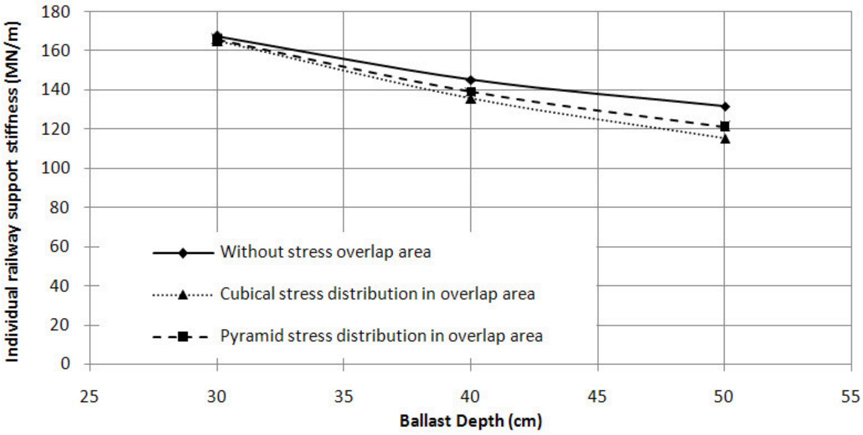

Fig. 5. Individual railway support stiffness versus ballast depth

Tab. 2. Equations of the support stiffness based on the ballast depths

Derived Stiffness	Equation	R-squared value
Without stress overlap area	$K = 830.3(BD)^{-0.47}$	$R^2 = 0.998$
With stress overlap area $\beta = 0$ (Cubical stress distribution)	$K = 1794.(BD)^{-0.70}$	$R^2 = 0.999$
With stress overlap area $\beta \neq 0$ (Pyramid stress distribution)	$K = 1334.(BD)^{-0.61}$	$R^2 = 1$

* In this table, "K" and "BD" are support stiffness (MN/m) and ballast depths (cm), respectively.

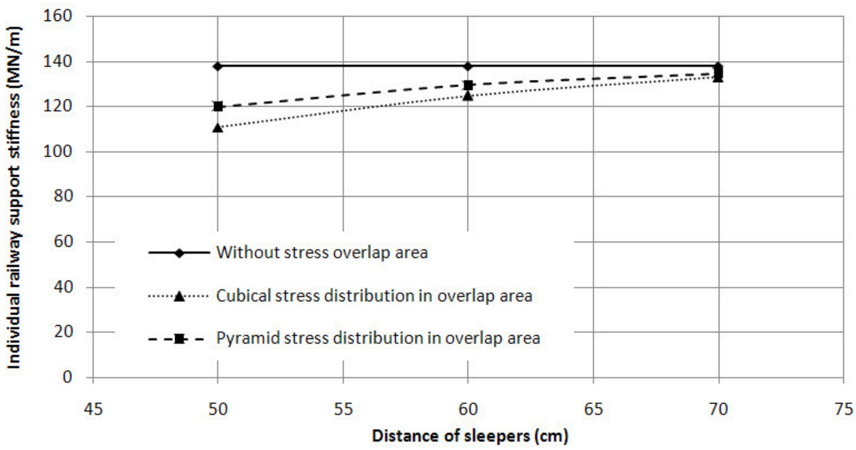

Fig. 6. Individual railway support stiffness versus sleeper distances

Tab. 3. Equations of support stiffness based on the distance of the sleepers

Derived Stiffness	Equation	R-squared value
Without stress overlap area	$K = 137.8$	$R^2 = 1$
With stress overlap area $\beta = 0$ (Cubical stress distribution)	$K = 13.42(DS)^{0.541}$	$R^2 = 0.984$
With stress overlap area $\beta \neq 0$ (Pyramid stress distribution)	$K = 31.17(DS)^{0.345}$	$R^2 = 0.983$

* In this table, "K" and "DS" are support stiffness (MN/m) and distance of sleepers (cm) respectively.

varies from 50 to 70 cm [16]. The calculated individual support stiffness in the railway track for various sleeper geometries is presented in Fig. 7. Figs. 7A, 7B and 7C are the individual support stiffness in the railway track for ballast depths of 30, 40 and 50 cm, respectively. In all presented results in this section, input parameters $\rho_b = 1800\,\text{kg/m}^3$, $L_e = 1.16\,\text{m}$, $\alpha = 35^o$, and $E_b = 110\,\text{MPa}$ have been utilized [16]. Morover, it should be emphasized that all coming results are calculated based on the pyramid model equations considering the stress overlap area (OAP).

From Fig. 7, it can be understood that the individual support stiffness in railway track rises by increasing the distance of the sleepers and decreasing the ballast depth for any width of the sleeper. Also, by increasing the width of the sleepers, the support stiffness increases. It is also revealed that the variations of the calculated track stiffness for the greater ballast depths are higher than those achieved for the ballast depth of 30 cm. The regression equations of the support stiffness and sleeper width are presented in Table 4 for various ballast depths.

From the results in Table 4, it is deduced that the equations for the support stiffness (K) based on the width of the sleepers (WD) are linear form (K = a.(WD) + b). In this equation, the coefficient "a" for each ballast depth increases by increasing the distance of the sleepers. Also, for the same distance of the sleepers, this coefficient decreases by increasing the depth of the ballast.

5 Modeling of the railway track and the vehicle

The model for the railway track is considered as a beam on viscoelastic supports. The viscoelastic supports are considered in the location of the sleepers. It should be considered that the stiffness of the support points is added to the main diagonal of the stiffness matrix. Customarily, for the simulation of the railway vehicle, its' components are modeled as lumped masses. Also, for defining the force vector, the location of the moving load is calculated. The rail points' forces are then calculated based on the shape functions. In what continues, the railway track model under the moving vehicle is verified.

6 Verification of the vechile-track models

In order to verify the numerical results of the present study, the models proposed by Lei and Zhang [12] and Koh et al. [13] are used.

In the present numerical study, a railway track with discrete viscoelastic supports is studied. The schematic for such a model is presented in Fig. 8. The railway vehicle with three degrees of freedom including the carbody, the bogie and the wheelset masses travels along the railway track with discrete supports. The system degrees of freedom are presented in a vector form in Eq. (14).

$$\{Z\} = [Z_c, Z_t, Z_w]^T \tag{14}$$

The railway track and the vehicle particulates are presented in Table 5.

The calculated vertical displacement versus the track position and the results from Lei and Zhang [12] and Koh et al. [13] are presented in Fig. 9.

Comparing the numerical results from this research with those that were reported by Lei and Zhang [12] and Koh et al. [13] it is concluded that the results are comparable. Also, the responses of present study are in good agreement with the previous ones. It is therefore concluded that the simulation of the railway track is satisfactory and the results are verified. The individual railway support stiffness for various sleeper geometries were obtained in section 4 and in continue, the behaviour of the railway tracks are investigated due to their effects in the next section.

7 The effects of the various sleeper geometries on the behavior of the railway track

Having estimated the individual railway support stiffness for various sleeper geometries, their effects on the behavior of the railway tracks are also investigated in this section. Fig. 10 depicts the ratio of the railway track vertical displacement to the vehicle load for various sleeper geometries and different ballast depths.

From Fig. 10, the ratio of the railway track vertical displacement to the vehicle load increases by incresing the distance of the sleepers. Also, it decreases by increasing the sleeper widths. By increasing the ballast depths, this ratio increases and the differences between these ratios for a certain sleeper distance reduce. The construed equations for the railway track vertical displacement to the vehicle load according to the distance of the sleepers for the different sleeper geometries are illustrated in Table 6.

From Table 6, the equation representing the behavior of the railway track vertical displacement to the vehicle load (DL)

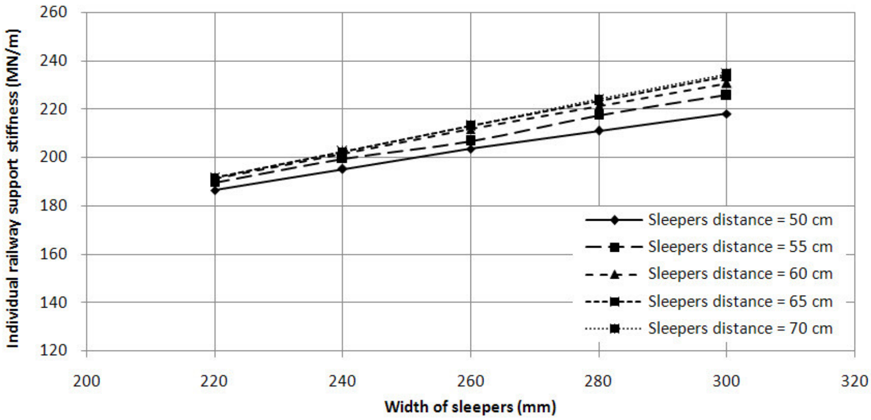

A) Ballast depth 30 cm

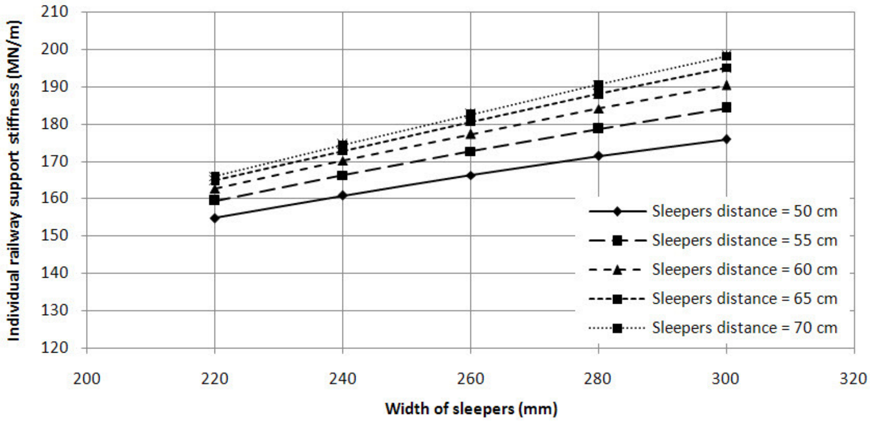

B) Ballast depth 40 cm

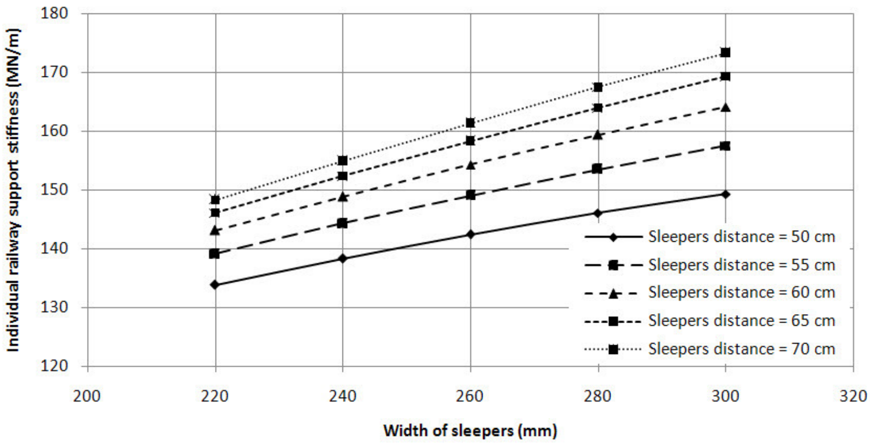

C) Ballast depth 50 cm

Fig. 7. Individual support stifness in the railway track for various sleeper geometries and ballast depths

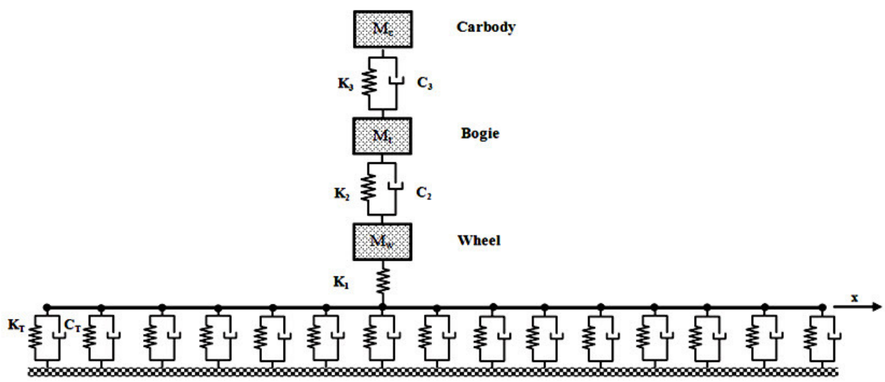

Fig. 8. The railway track and the vehicle model for verifying the results

Tab. 4. The equation coefficients for the support stiffness based on the width of the sleepers

Ballast Type	Depth of ballast (cm)	Distance of sleepers (cm)	Linear Equation "K = a.(WD) + b" "a"	"b"	R-squared value
BT 1	30	50	0.39	100.3	$R^2 = 0.997$
		55	0.45	90.6	$R^2 = 0.997$
		60	0.49	83	$R^2 = 0.999$
		65	0.53	76.4	$R^2 = 0.999$
		70	0.54	73	$R^2 = 1$
BT 2	40	50	0.26	97.2	$R^2 = 0.997$
		55	0.31	91.9	$R^2 = 0.998$
		60	0.35	86.8	$R^2 = 0.998$
		65	0.38	82.2	$R^2 = 0.999$
		70	0.4	78.1	$R^2 = 0.999$
BT 3	50	50	0.19	91.6	$R^2 = 0.996$
		55	0.23	88.7	$R^2 = 0.997$
		60	0.26	85.6	$R^2 = 0.998$
		65	0.29	82.5	$R^2 = 0.999$
		70	0.31	79.6	$R^2 = 0.999$

* "K" and "WD" are the support stiffness (MN/m) and the width of the sleepers (cm), respectively.

Tab. 5. The railway track and the vehicle particulates used for the verification purposes

Parameters	Values	Parameters	Values
Vehicle mass (Mc)	3500 kg	Vehicle speed (V)	72 km/h
Bogie mass (M_t)	250 kg	Rail mass (m_r)	60 kg/m
Wheel mass (M_w)	350 kg	Young's modulus of rail (E_r)	2×10^5 MPa
Primary suspension stiffness (K_2)	1.26×10^3 kN/m	Inertia moment of rail (I_r)	3.06×10^{-5} MPa
Secondary suspension stiffness (K_3)	1.41×10^2 kN/m	Distance of sleepers (L_s)	0.5 m
Primary suspension damping (C_2)	7.1 kNs/m	Rail length (L_r)	20 m
Secondary suspension damping (C_3)	8.87 kNs/m	Track damping (C_T)	4.9 kNs/m^2

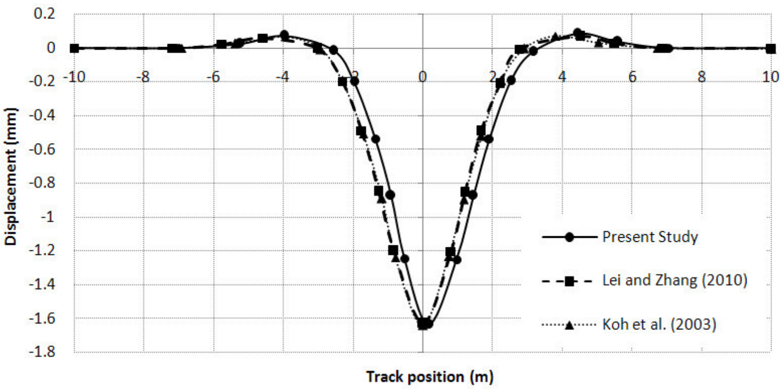

Fig. 9. The vertical displacement of the railway track based on the track position

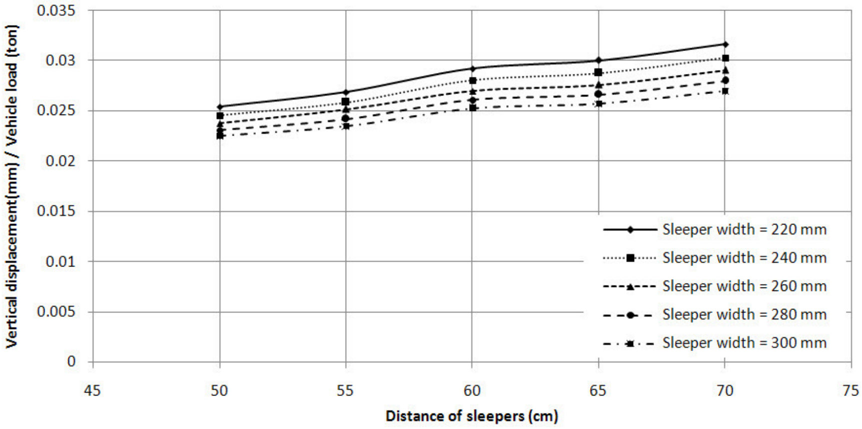

A) Ballast depth of 30 cm

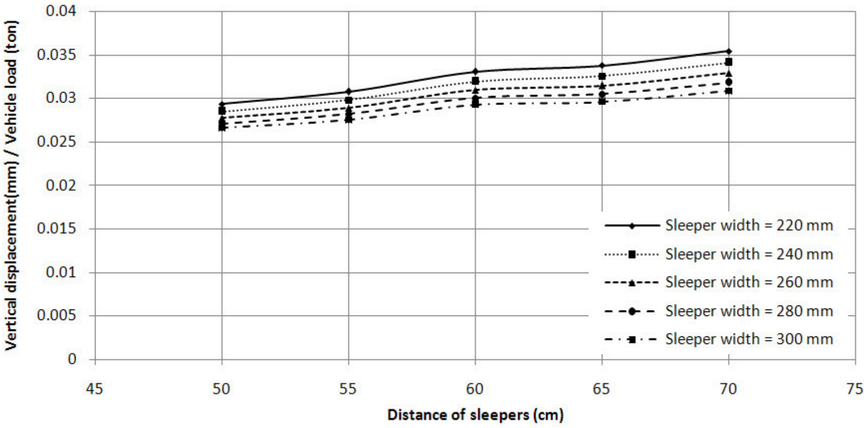

B) Ballast depth of 40 cm

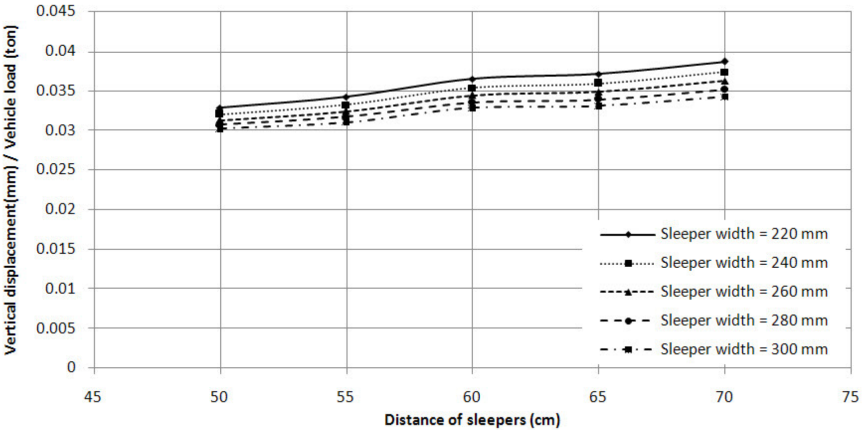

C) Ballast depth of 50 cm

Fig. 10. The ratio of the railway track vertical displacement to the vehicle load based on the various sleeper geometries for different ballast depths

Tab. 6. The equation coefficients for the railway track vertical displacement to the vehicle load based on the distance of the sleepers

Depth of ballast (cm)	Width of sleepers (mm) (mm)	Logarithmic Equation "DL = a.ln(DS) + b"		R-squared value
		"a"	"b"	
30	220	0.018	- 0.047	$R^2 = 0.987$
	240	0.017	- 0.042	$R^2 = 0.986$
	260	0.015	- 0.037	$R^2 = 0.988$
	280	0.014	- 0.033	$R^2 = 0.981$
	300	0.013	- 0.029	$R^2 = 0.979$
40	220	0.018	- 0.041	$R^2 = 0.985$
	240	0.016	- 0.036	$R^2 = 0.982$
	260	0.015	- 0.031	$R^2 = 0.979$
	280	0.013	- 0.027	$R^2 = 0.978$
	300	0.012	- 0.022	$R^2 = 0.972$
50	220	0.017	- 0.035	$R^2 = 0.982$
	240	0.016	- 0.030	$R^2 = 0.980$
	260	0.014	- 0.026	$R^2 = 0.977$
	280	0.013	- 0.021	$R^2 = 0.973$
	300	0.012	- 0.017	$R^2 = 0.967$

* "DL" and "DS" are the ratio of the railway track vertical displacement to the vehicle load and the distance of the sleepers (cm), respectively.

based on the distance of the sleepers (DS) is in the logarithmic form (DL = a.ln(DS) + b). In this equation, the coefficient "a" for each ballast depth decreases by increasing the width of the sleepers.

8 Conclusions

This article proposed models that can be effectively used in order to calculate the individual support stiffness in the railway tracks. It is based on the pyramid stress distribution model for WOA, OAP and OAC conditions. The railway track was simulated by using the finite element method. The results were verified by comparing them with the results that were reported by other researchers in this filed. Finally, the effects of individual railway support stiffness on the track deflection for various sleeper geometries were investigated. The most valuable findings of the present study can be summarized as;

1 Three different equations were derived for assessing the individual track stiffness using the pyramid model. These cover the WOA model for the cases of having no stress overlap area in the adjacent sleepers, OAP model for considering the stress overlap area between adjacent sleepers with pyramid stress distribution and OAC model for the cases with stress overlap area between adjacent sleepers with cubical stress distribution.

2 Due to the increasing of the ballast depths from 30 to 50 cm, the individual railway support stiffness decreases 21, 27 and 30 percent for WOA, OAP and OAC conditions, respectively. Moreover, by decreasing the ballast depths, the resulted support stiffness by WOA, OAP and OAC models converges to a constant value.

3 The correlated equations between the results of individual support stiffness (K) and the ballast depths (BD) are in the power form ($K = a.(BD)^b$). The average R-value for these equations is 0.999.

4 For WOA condition, the variation of the sleepers distance has no effect on the support stiffness. However, increasing the distance of the sleepers from 50 to 70 cm, increases in the support stiffness amounting to 12 and 20 percent, for OAP and OAC conditions, respectively, were observed. Moreover, by increasing the distance of the sleepers, the resulted support stiffness by OAP and OAC models converges to a constant value.

5 Same as the ballast depth, the correlated equations between the results of the individual support stiffness (K) and the distance of the sleepers (DS) are in the power form ($K = a.(DS)^b$). The average R-value for these equations is 0.989.

6 By increasing the distance of sleepers from 50 to 70 cm for the sleeper width of 220 mm, the individual support stiffness in railway track increases by 3, 7 and 11 percent for the ballast depths of 30, 40 and 50 cm, respectively. Also, it increases by 8, 13 and 16 percent for the ballast depths of 30, 40 and 50 cm by increasing the distance of the sleepers from 50 to 70 cm for the sleeper width of 300 mm, respectively.

7 The correlation equations between the individual support stiffness (K) and the sleeper width (WD) is in the linear form (K = a.(WD) + b). The average R-value for these equations is 0.998.

8 For the ballast depth of 40 cm, the ratio of the railway track vertical displacement to the vehicle load increases by 21 and 16 percent when incresing the distance of the sleepers from 50 to 70 cm for sleeper widths of 220 and 300 mm, respectively.

9 The correlated equations between the ratio of the railway track vertical displacement to the vehicle axle load (DL) and

the distance of the sleepers (DS) are in the logarithmic form $(DL = a.\ln(DS) + b)$. The average R-value for these equations is 0.980.

References

1 **Szépe F**, *Load distribution capacity of railway superstructure*, Periodica Polytechnica Civil Engineering, **35**(3-4), (1991), 205–224.

2 **Zakeri JA, Xia H**, *Sensitivity analysis of track parameters on train-track dynamic interaction*, Journal of Mechanical Science and Technology, **22**(7), (2008), 1299–1304, DOI 10.1007/s12206-008-0316-x.

3 **Zoller V, Zobory I**, *Three-layer in-plane dynamical track model for metro applications*, Periodica Polytechnica Civil Engineering, **58**(4), (2014), 335–338, DOI 10.3311/PPci.7638.

4 **Kerr AD**, *On the determination of the rail support modulus K*, International Journal of Solids and Structures, **37**(32), (2000), 4335–4351, DOI 10.1016/S0020-7683(99)00151-1.

5 **Kerr AD**, *Fundamentals of railway track engineering*, Simmons-Boardman Books, 2003.

6 **Zhai WM, Wang KY, Lin JH**, *Modelling and experiment of railway ballast vibrations*, Journal of Sound and Vibration, **270**(4-5), (2004), 673–683, DOI 10.1016/S0022-460X(03)00186-X.

7 **Puzavac L, Popovic Z, Lazarevic L**, *Influence of track stiffness on track behavior under vertical load*, Scientific Journal on Traffic and Transportation Research, **24**(5), (2012), 405–412, DOI 10.7307/ptt.v24i5.1176.

8 **Breul P, Saussine G**, *On site mechanical characterization of the ballast state*, Periodica Polytechnica Civil Engineering, **55**(1), (2011), 31–38, DOI 10.3311/pp.ci.2011-1.04.

9 **Zakeri JA, Abbasi R**, *Field investigation of variation of rail support modulus in ballasted railway track*, Latin American Journal of Solids and Structures, **9**(6), (2012), 643–656, DOI 10.1590/S1679-78252012000600002.

10 **Zakeri JA, Esmaeili M, Mosayebi SA, Abbasi R**, *Effects of vibration in desert area caused by moving trains*, Journal of Modern Transportation, **20**(1), (2012), 16–23, DOI 10.1007/BF03325772.

11 **Esmaeili M, Zakeri JA, Mosayebi SA**, *Effect of sand-fouled ballast on train-induced vibration*, International Journal of Pavement Engineering, **15**(7), (2014), 635–644, DOI 10.1080/10298436.2013.818146.

12 **Lei X, Zhang B**, *Influence of track stiffness distribution on vehicle and track interactions in track transition*, Proceedings of the Institution of Mechanical Engineers, Part F: Journal of Rail and Rapid Transit, **224**(6), (2010), 592–604, DOI 10.1243/09544097JRRT318.

13 **Koh CG, Ong JSY, Chua DKH, Feng J**, *Moving element method for train-track dynamics*, International Journal for Numerical Methods in Engineering, **56**(11), (2003), 1549–1567, DOI 10.1002/nme.624.

14 **Ahlbeck DR, Meacham HC, Prause RH**, *The development of analytical models for railroad track dynamics*, Railroad Track Mechanics and Technology, In: **Kerr AD** (ed.), Railroad Track Mechanics and Technology; Princeton, New Jersey, 1975, pp. 239–263.

15 **Selig ET, Waters JM**, *Track Geotechnology and Substructure Management*, Thomas Telford; London, 1994.

16 *Leaflet No. 301, Technical and general specification of ballasted railway*, Management and Planning Organization of Iran; Tehran, Iran, 2002.